IDEAL CYCLE THERMODYNAMIC ANALYSIS FOR GAMMA-TYPE STIRLING ENGINE

Jufrizal[1,2], F. H. Napitupulu[1,*], Ilmi[1], H. Ambarita[1] and M. Meliala[2 1]

[1]Mechanical Engineering, Universitas Sumatera Utara, Medan, Indonesia

[2]Mechanical Engineering, Universitas Medan Area, Medan, Indonesia

Corresponding Author's Email: farel@usu.ac.id

Article History: Received 3 August 2021; Revised 1 October 2022; Accepted 1 December 2022

ABSTRACT: The first-generation gamma-type Stirling engine prototype, intended for micro combined heat and power applications, was manufactured and tested in 2018. Still, the findings were not promising due to its low performance. The goal of this research is to improve the performance of the gamma-type Stirling engine by using the ideal cycle thermodynamic analysis approach to plan more comprehensively. The research approach employed in this study is an experiment that begins with the design, fabrication, testing, and evaluation of the Stirling engine's components. With air as the working fluid, the second-generation gamma-type Stirling engine was created and tested. The maximal volume of this engine is 0.000201 m^3. The heat source employed in the test had an average temperature of 674^{o}C. The results showed that, while not dramatically, the performance engine improved. The value of thermal efficiency, engine speed, and power output all increased. The average thermal efficiency is 24.6%. Meanwhile, the engine speed and power generated averaged 415 rpm and 37.9 W. This increase in performance is a compelling reason to continue to develop the gamma-type Stirling engine in the future.

KEYWORDS: *Gamma-type Stirling engine, ideal cycle thermodynamic, performance*

1.0 INTRODUCTION

The issue of saving and using environmentally friendly energy sources encourages engineers worldwide to continue developing thermal energy conversion systems that have higher efficiency. This problem occurs as a result of rising global energy consumption and increasing environmental impact daily. Indonesia's energy demand is expected to rise through 2050, owing to economic growth, population, energy pricing, and government regulations. The annual growth rate of total energy demand is 5.3 per cent. Energy demand is expected to rise from 795 million BOE in 2016 to 4,569 million Barrels of Oil Equivalent (BOE) in 2050 [1]. As a result of these facts, it is vital to consider energy-saving initiatives in various areas [2-5]. Another way is to build a combined heat and power (CHP) system, which uses only one fuel and produces both heat and electricity simultaneously. A Stirling engine is typically utilized in a micro-scale CHP system.

The Stirling engine was chosen for development because it can run on various heat sources, including renewable fuels, waste heat, and solar energy. Controllable combustion, long life, extended maintenance time, high efficiency, noise, low vibration, and low emissions are all advantages of the Stirling engine [6-12]. Based on their configuration, the Stirling engine is divided into three categories: alpha (α), beta (β), and gamma (γ). Each configuration has its own set of advantages and disadvantages. An overview of the development of several gamma-type Stirling engine models from time to time can be seen in Figure 1 [13-26] . Because of the same thermodynamic advantages as the design beta, the authors are more interested in constructing a gamma-type Stirling engine in this study [27]. Its construction is simpler, and it can move at low-temperature differences.

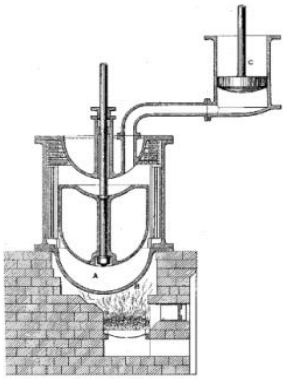

Robert and J Stirling-1827

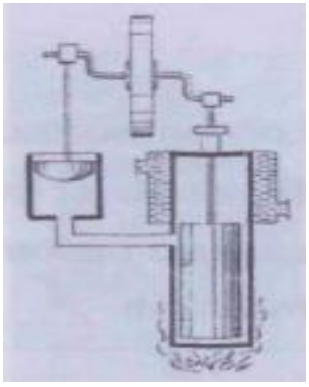

Heindrici-1884

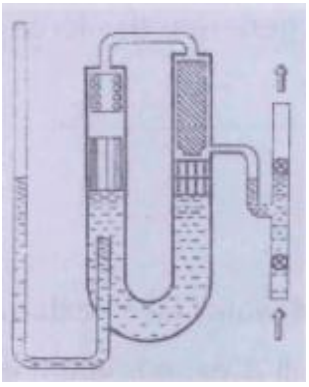

West-1970

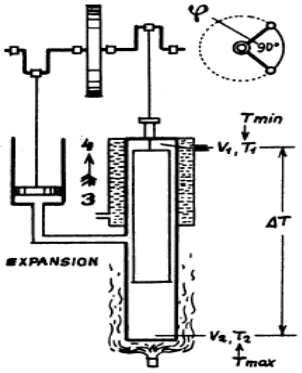

Kolin et al.-2000

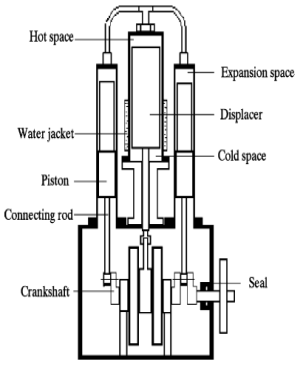

Cinar and Karabulut-2005

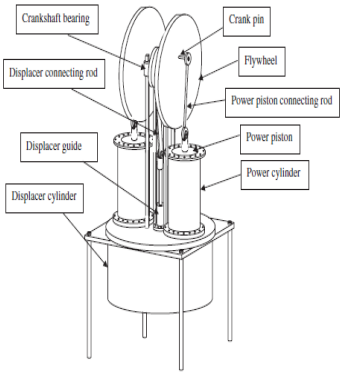

Kongtragool et al-2007

Figure 1: Description of the development of the Stirling gamma type engine model

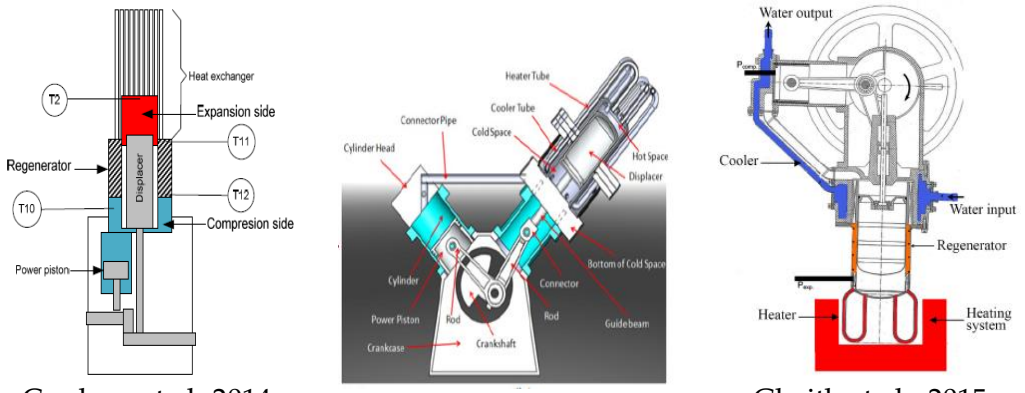

Cardozo et al.-2014 Damirchi et al.-2015 Gheith et al..-2015

Figure 1: Description of the development of the Stirling gamma type engine model (continued)

The first generation gamma-type Stirling engine was manufactured and tested in 2018. This engine uses air as the working fluid and has a compression volume of 106 cm^3. The resultant pressure is 1.82 bar, according to the calculations. With a thermal efficiency of 18.78%, the best engine capability is attained at 242.6 rpm and 12.9 W [8]. Based on this investigation, it has been discovered that the engine performance is still relatively low, necessitating a more detailed design and analysis before the engine can be manufactured. This research aims to use an ideal cycle thermodynamic analysis approach to examine the prototype of the 2nd generation gamma type Stirling engine.

2.0 METHODOLOGY

2.1 Ideal Stirling Cycle

Robert Stirling invented the Stirling engine in Scotland in 1816, about 80 years before the Diesel engine, and it was a commercial success until the early 1900s [27]. Since then, several methods for analyzing the Stirling engine have been devised, ranging from simple to complex. The Stirling engine thermodynamic analysis model has been widely given in the literature, with varied assumptions. Stirling engine modelling can be divided into three categories. The ideal analysis calculates the theoretical performance of an engine with a zero or infinite convection heat transfer coefficient [28-30]. The combined analysis is based on the smooth discretization of engines in different control volumes, taking into account all major disadvantages [27]. The most basic model in the calculation and analysis of the Stirling engine is the ideal Stirling cycle based on the thermodynamic solution approach.

The ideal Stirling engine cycle is shown in the P-V and T-S diagram in Figure 2 [27]. The ideal Stirling cycle consists of four processes, namely compression, regeneration, expansion, and regeneration.

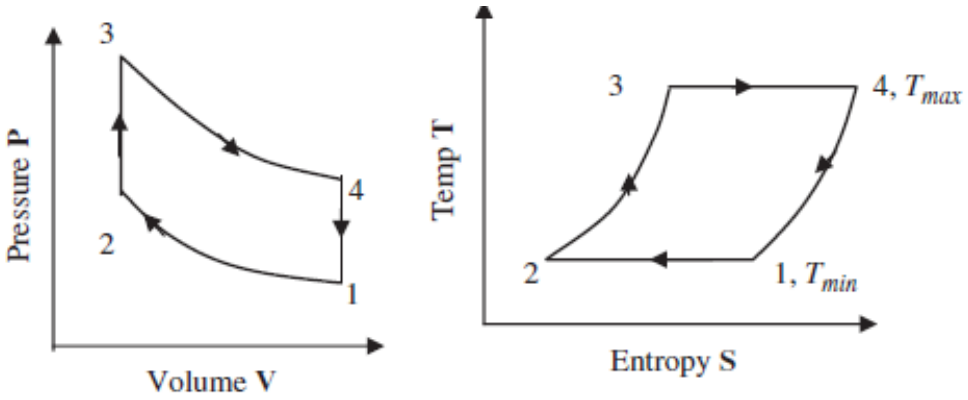

Figure 2: Ideal Stirling cycle P-V and T-S

Process 1-2 is an isothermal compression process in which heat is transferred from the working fluid to the outer fin at a temperature of T_{min}. This procedure is defined by the piston compressing the working fluid to increase the pressure from P_1 to P_2. Because heat flows from the cooler to the environment, the temperature remains constant.

Process 2-3 is an isochoric regeneration process in which heat is transferred from the regenerator matrix to the working fluid. The working fluid is moved from the compression chamber to the expansion chamber via the porous regenerator, with the two pistons running simultaneously. The piston moves towards the regenerator and the displacer away from the regenerator so that the volume between the pistons remains constant. The working fluid has been preheated in the regenerator. The working fluid temperature increases from T_{min} to T_{max} by transferring heat from the regenerator matrix to the working fluid.

Process 3-4 is an isothermal expansion process, transferring heat to the working fluid at temperature T_{max} from the external heat source. This process occurs when the displacer moves away from the regenerator towards the lower dead centre while the compression piston remains at the top dead centre adjacent to the regenerator. Pressure decreases as volume increases. The temperature remains constant by adding heat to the system from the heater.

Process 4-1 is an isochoric regeneration process, transferring heat from the working fluid to the regenerator matrix. This process occurs when both pistons move simultaneously to transfer the working fluid from the expansion chamber to the compression chamber through the regenerator at a constant volume. Heat is transferred from the working fluid to the regenerator matrix. During the working fluid flow through the regenerator, heat is transferred from the working fluid to the regenerator matrix, which reduces the working fluid temperature to T_{min}.

The ability of the Stirling engine is determined by several parameters like the Otto and Diesel engines, such as thermal efficiency, engine speed, torque, and power produced. Especially for the Stirling engine, another parameter that shows capability is the

temperature difference on the hot and cold sides. The thermal efficiency of the ideal Stirling cycle can be calculated by equation (1) [24].

$$\eta_{th} = 1 - \frac{T_1}{T_3} = 1 - \frac{T_{min}}{T_{max}} = 1 - \frac{T_C}{T_E} \quad (1)$$

where

$T_1 = T_2 = T_{min} = T_C$ = Compression space temperature

$T_3 = T_4 = T_{max} = T_E$ = Expansion space temperature

The first stage for designing the Stirling engine is to determine the diameter and stroke of the piston and calculate the stroke volume for the displacer, V_{SE}, and stroke volume for the piston, V_{SC} using equations (2) and (3) [31].

$$V_{SE} = \frac{\pi}{4} \times \left(B_{dp}\right)^2 \times S_{dp} \quad (2)$$

$$V_{SC} = \frac{\pi}{4} \times \left(B_{pp}\right)^2 \times S_{pp} \quad (3)$$

Where B_{dp} and B_{pp} are the diameters of the displacer and piston. S_{dp} and S_{pp} are displacer and piston steps from top dead centre to bottom dead centre.

The volume of expansion space (V_E), compression volume (V_C), and total volume (V) can be calculated by equations (4), (5), and (6) [24,31].

$$V_E(\alpha) = \frac{V_{SE}}{2}[1 - COS(\alpha)] \quad (4)$$

$$V_C(\alpha) = \frac{V_{SE}}{2}(1 + COS\,\alpha) + \frac{V_{SC}}{2}[1 - COS(\alpha - \varphi)] \quad (5)$$

$$V(\alpha) = V_E + V_D + V_C \quad (6)$$

Where α is the crank angle that is used to determine the expansion volume and compression volume at different crank angles, which are 0^o to 360^o. Whereas φ is the difference in angle between the displacer and the power piston, it is called the phase angle. This phase angle is 90° on the gamma-type Stirling engine, which means that the piston displacer and power piston will move sinusoidally with each other.

In ideal conditions, all working fluids are located in the expansion and compression chamber. But because most Stirling engines have a dead volume (V_D) of 40-50% of the total volume [23]. V_D is the sum of the dead volume in the expansion cylinder (V_{DE}) and compression (V_{DC}) and the regenerator chamber (V_R). This dead volume causes a decrease in pressure and total efficiency. V_D is calculated by equation (7) [31].

$$V_D = V_{DE} + V_R + V_{DC} \quad (7)$$

Furthermore, the important parameter of the Stirling engine is the compression ratio. The compression chamber volume consists of two parts because the gamma-type Stirling engine uses the compression chamber piston and the displacement to suppress the working fluid. The Stirling engine compression ratio is a function of the crank angle. Because the heat exchanger and regenerator have a large dead volume, the Stirling engine only achieves a

compression ratio of around 2-3, while the Otto and Diesel engines have a value of around 9-22 [24]. The compression ratio on the Stirling engine can be calculated by equation (8) [24].

$$\varepsilon = 1 + \frac{V_{SC}}{V_{SE}+V_D} \tag{8}$$

The work generated in the ideal Stirling cycle is represented by isothermal compression processes and isothermal expansion processes. Both of these processes can be calculated using a thermodynamic analysis approach. The isothermal compression process of the working fluid between points 1 to 2 in Figure 2 involves the transfer of heat from the working fluid to the coolant/fin at T_{min}. Pressure, heat, and work in the 1-2 process, then equations (9) and (10) apply [27].

$$P_2 = \frac{P_1 V_1}{V_2} = P_1 r_v \tag{9}$$

and

$$W_c = Q_{1-2} = Q_{out} = m \times R \times T_1 \times \ln\left(\frac{1}{r_v}\right) \tag{10}$$

The isothermal expansion process between points 3 to 4 in Figure 2 is characterized by the temperature being kept constant by adding heat to the system from an external source at T_{max}. Pressure, heat, and work in the 3-4 process, then equations (11) and (12) apply [27].

$$P_4 = \frac{P_3 V_3}{V_4} = P_3\left(\frac{1}{r_v}\right) \tag{11}$$

and

$$W_E = Q_{3-4} = Q_{in} = m \times R \times T_3 \times \ln\left(\frac{1}{r_v}\right) \tag{12}$$

where r_v is the ratio of expansion and compression volume assuming $V_2 = V_3 = V_{min}$ and $V_1 = V_4 = V_{max}$ calculated by equation (13) [27].

$$r_v = \frac{V_1}{V_2} = \frac{V_4}{V_3} \tag{13}$$

The mass of the working fluid is calculated using the ideal gas equation approach (14).

$$m = \frac{P_1 \, x \, V_1}{R \, x \, T_1} \tag{14}$$

R is the constant gas value, the R-value of several working fluids often used in Stirling engines as shown in Table 1 [32].

Table 1. Gas constant properties

Working fluids	Air	Helium, He	Hydrogen (normal), H_2
R, kJ/kg·K	0.2870	2.0769	4.1240

While processes 2-3 and 4-1 are isochoric regeneration, the pressure in these two processes can be calculated by equations (15) and (16) [27].

$$P_3 = \frac{P_2 T_3}{T_2} = \frac{P_2}{\tau} \quad (15)$$

and

$$P_1 = \frac{P_4 T_4}{T_1} = P_1 \tau \quad (16)$$

The work performed by the cycle according to the first law of thermodynamics is calculated by equation (17).

$$W_{net} = -[Q_{1-2} + Q_{3-4}] = Q_{in} - Q_{out} \quad (17)$$

The power generated in the ideal Stirling cycle can be calculated using equations (18) and (19). n is the rotational speed of the Stirling engine.

$$P = n \times W \quad (18)$$

or

$$P = n.\frac{1}{60} W \quad (19)$$

2.2 Experimental Setup

Tests are carried out in research to obtain experimental data. The variables measured in this study include the temperature profile, namely the temperature of the heat source (T_S), the temperature on the hot side (T_E), the temperature on the cold side (T_C), and the temperature in the cooling water (T_W). Besides, the engine speed is also measured at the flywheel. An illustration of the tests that will be carried out in the research is shown in Figure 3. Apart from the Stirling engine, several measuring instruments are needed to obtain the research variables measured. The temperature controller used is Autonics T4WM. The T4WM digital temperature indicators can display up to 5 input channels from separate sensors. The units feature high accuracy measurement and display of ± 0.5%, and users can select auto or manual channel switching based on preference. The auto-switching time interval can be set up to 10 seconds. While the thermocouple used is type K (Chromel (Ni-Cr alloy)/Alumel (Ni-Al alloy) with a temperature range of −200°C to +1200°C. To measure engine rotational speed (n), a Krisbow tachometer type KW 06-563 is used digital contact/non-contact tachometer. This tachometer has an accuracy ± (0.05% + 1 digit) with a measuring range of 2 to 99.999 rpm for non-contact conditions.

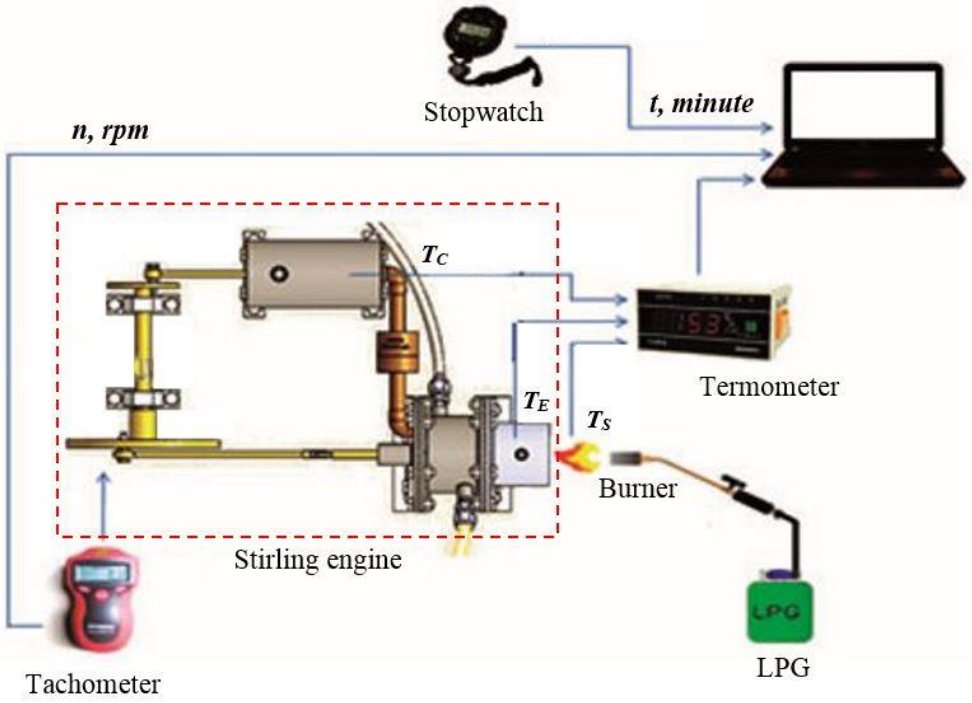

Figure 3: Experimental setup

The fuel used in this test is 3 kg liquid petroleum gas (LPG) from Pertamina gas products. The calorific value and density of LPG are 48.8 MJ/kg and 1.71 kg/m^3, respectively [33]. The working fluid used is air under ambient conditions. As the working fluid for the Stirling engine, the air is used with the initial conditions. The pressure and temperature are the same as the environmental conditions.

3.0 RESULTS AND DISCUSSION

3.1 Design and Manufacturing Stirling Engine

The initial parameters as a reference for designing the Stirling engine have been determined and calculated by equations (2) and (3). The results are presented in Table 2.

Table 2: Parameters Stirling engine

B_{dp}, m	S_{dp}, m	V_{SE}, m^3	B_{pp}, m	S_{pp}, m	V_{SC}, m^3
0.056	0.04	0.0000985	0.048	0.05	0.0000905

Furthermore, the dead volume calculation is carried out in the expansion, compression, and regenerator pipe sections based on the measurement results and calculations on the Stirling engine components that have been made. At the same time, the compression ratio is obtained after being calculated by equation (8).

Table 3. Dead volume and compression ratio

V_{DE} , m³	V_{DC} , m³	V_R , m³	V_D, m³	ε
0.00000246	0.00000181	0.00000763	0.00001191	1.82

The volume of expansion space, compression volume, and total volume, which is a function of the crank angle after being calculated by equations (4), (5), and (6), are then displayed in graphical form as in Figure 4. Figure 4 shows that the minimum total volume produced is 0.000110 m³ occurs at a 90° crank angle. While the maximum total volume occurs at the crank angle 270° is 0.000201 m³.

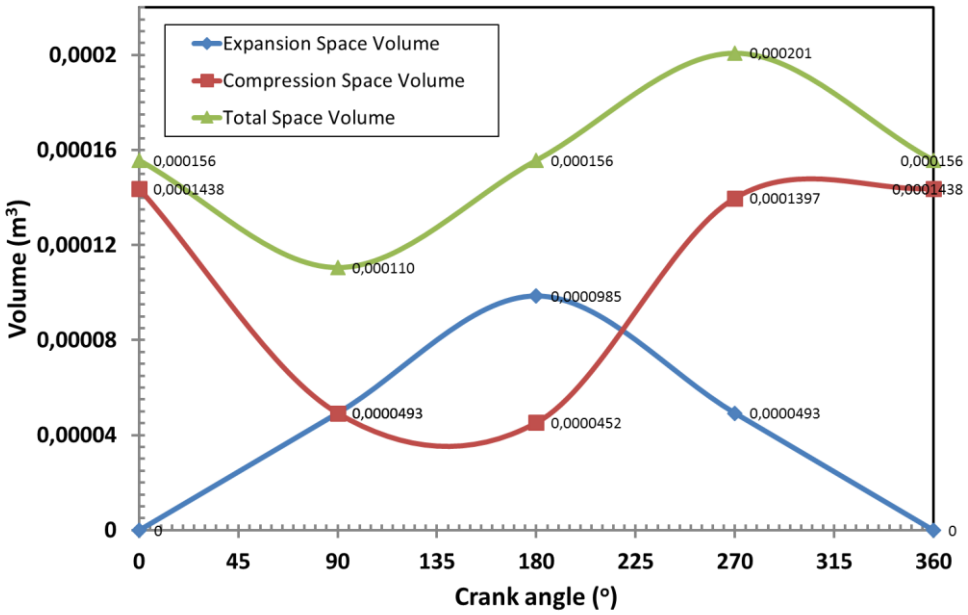

Figure 4: Volume as a function of the crank angle

Based on the data generated from the previous selection and calculation, the Stirling engine was built. The type of Stirling engine is gamma and is named mCHPSE-012019. The shape of the 2nd generation Stirling engine is as shown in Figure 5. The main components of the Stirling engine mCHPSE-012019 shown in Figure 5 include a heater (1), the cylinder and piston of displacer (2), the cylinder and piston of power piston (3), connecting rod (4), flywheel (5), and crankshaft (6).

The displacer cylinder is a part of the Stirling engine that receives hot air from the heater, which is then transferred to the power piston cylinder through the displacer piston. At the end of this displacer, there is a heater as a heater for the Stirling engine. The displacer cylinder is made using cast iron with a thickness of 3 mm, a length of 65 mm, and a diameter of 60 mm. This cylinder is equipped with a water jacket that functions as a coolant for the displacer cylinder with a length of 55 mm, an inner diameter of 66 mm, and an outer diameter of 76 mm. The displacer piston is a piston located in the displacer cylinder, which functions as a transfer of air from the hot side to the cold side. The displacer piston has a

gap with the cylinder wall, which functions as an alternating airflow. In this design, the piston and the cylinder wall difference is 2 mm from a predetermined difference of at least 1 mm. This difference of two mm is taken to compensate for the expansion of the piston when it receives heat. This piston is made of aluminium with a thickness of 1 mm, a length of 80 mm, and a diameter of 56 mm. The heater is the heat exchanger component in the Stirling engine. This component is located at the end of the displacer cylinder. The heater is made of copper with a thickness of 3 mm, a length of 60 mm, and a diameter of 60 mm.

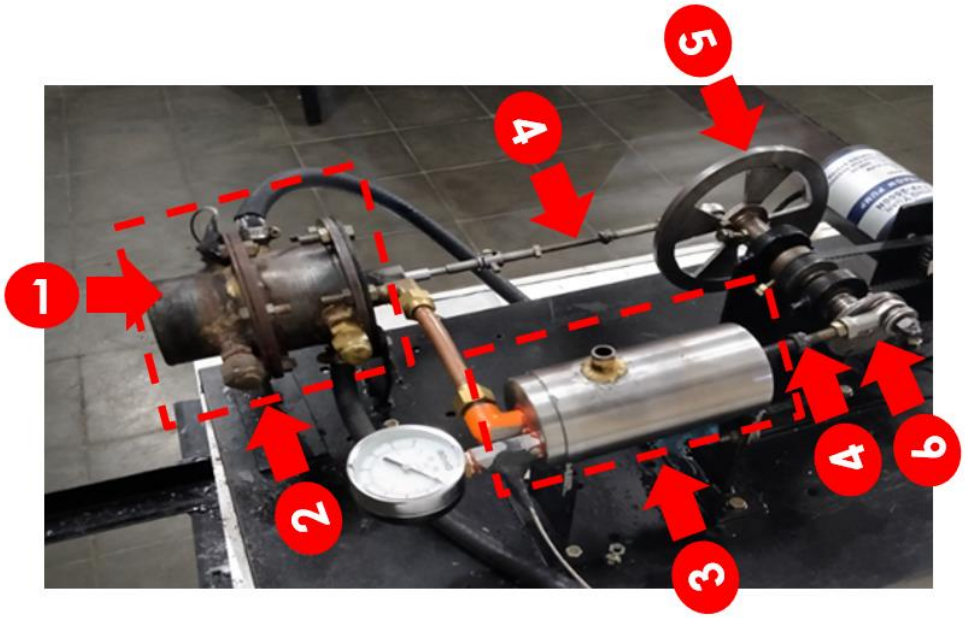

Figure 5: A gamma-type Stirling engine that has been manufactured

The power piston cylinder is a component of the Stirling engine on the cold side. This cylinder is made of cast iron with a thickness of 3 mm, a length of 120 mm, and a diameter of 48 mm. This cylinder is equipped with a water jacket that cools the power piston cylinder with a length of 117 mm, an inner diameter of 54 mm, and an outer diameter of 64 mm. The power piston is a component of the Stirling engine that functions to move power to the crankshaft. This piston is made of fibre with a diameter of 48 mm and a length of 40 mm. The crankshaft is a part of the Stirling engine, which functions to change the translational motion of the connecting rod into rotational motion. This shaft is made of cast iron with a length of 160 mm and a diameter of 15 mm. The flywheel is the inertia mass to which the piston and displacer are combined. There is only one force, and as long as it moves, the flywheel gets some energy as rotational kinetic energy; as a result, the flywheel speed will increase. The flywheel is made using cast iron with a flywheel size of 8 mm thick and 150 mm in diameter. The connecting rod is used to connect or as a liaison between the piston and the displacer and the flywheel to transmit power from the piston action in alternating movements between the displacer and piston when the Stirling engine is working. Connecting rods are made with a length of 208.5 mm and 167 mm.

3.2 Stirling Engine Testing

The temperature of T_S, T_E, T_C, and T_W was measured and recorded. Temperature data were recorded every 1 minute for 30 minutes and repeated three times during the test. The 3rd data from the test results are averaged, and the results are presented in graphical form in Figure 6.

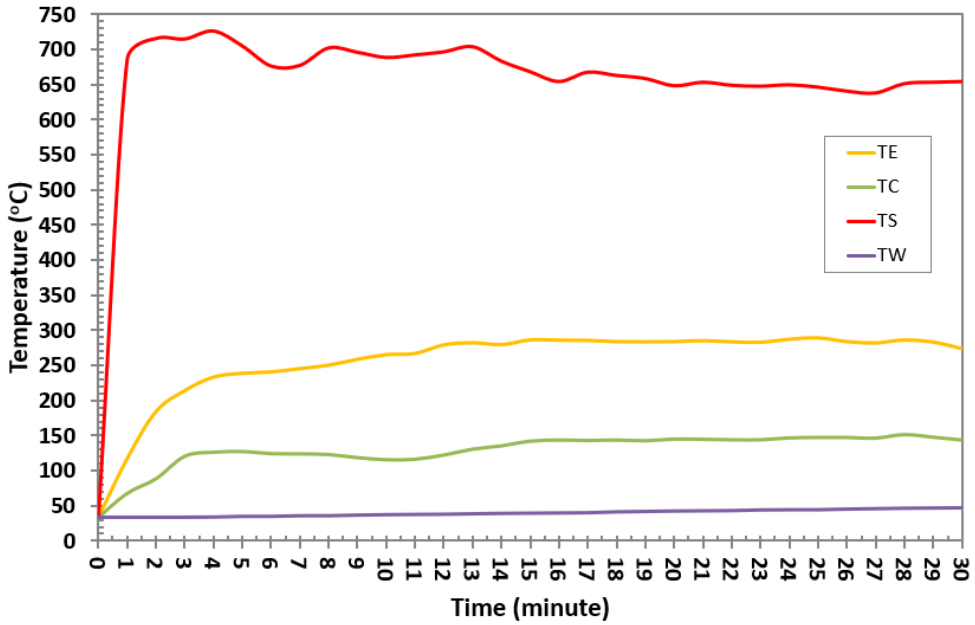

Figure 6: The average temperature profile of the Stirling engine for three times testing

Figure 6 shows that the graphs of heat source temperature (T_S), hot side temperature (T_E), and cold side temperature (T_C) have the same increase pattern during the test except that the cooling water temperature (T_W) is maintained between 33°C to 48°C. At the beginning of the process, there is high heat absorption by the working fluid through the heater on the hot side to the maximum temperature. The temperature at the beginning of the process is the same, which is 33°C. The heat source temperature in the first minute has a significant increase, from 33°C to 686°C, then only after that it starts to be almost constant in the range of 674°C. The average hot side temperature and cold side temperature are 264°C and 131°C. The temperature difference between the hot and cold sides is 132°C. Based on data on hot side temperature and cold side temperature, the thermal efficiency of the ideal Stirling cycle is obtained, which is calculated by equation (1) of 24.6%.

The pattern of increase that occurs in the graph of heat source temperature, hot side temperature, and cold side temperature also occurs at an engine rotational speed, as shown in Figure 7. The engine starts moving in the first minute with an initial speed of 70 rpm, and after that, the average is at 415 rpm. The speed of the Stirling engine is greatly influenced by the heat source temperature, hot side temperature, and cold side temperature. In Figures 6 and 7, it is also seen that the higher the difference in temperature on the hot side and the temperature on the cold side that enters the system, the engine rotation speed that occurs on the Stirling engine will increase. From the results of calculations using equations (10),

(12), (13), (14), (17), and (19), the average power generated by the Stirling engine is 37.9 W. The relationship between pressure and volume for an ideal cycle is shown in Figure 8.

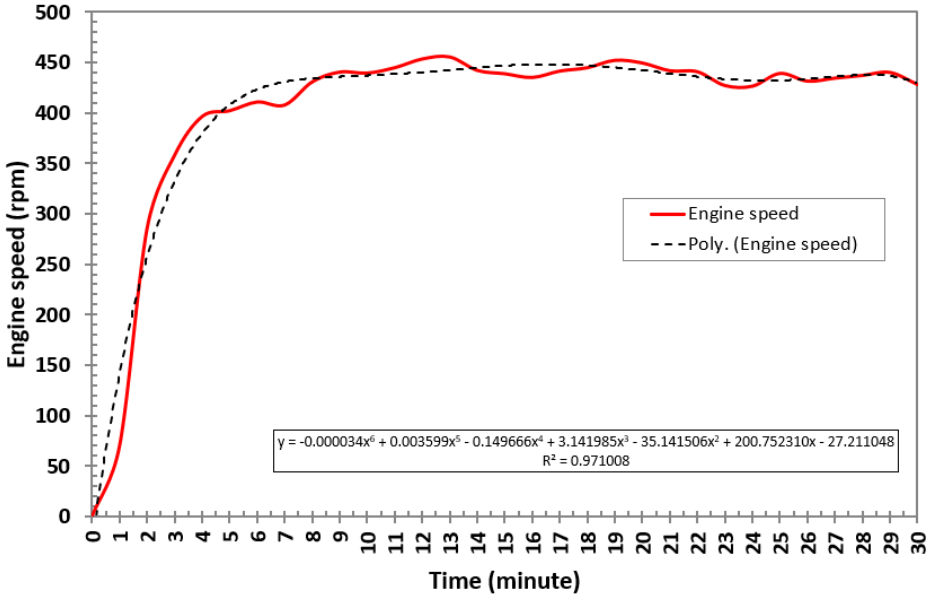

Figure 7: The average engine speed of the Stirling engine for three times testing

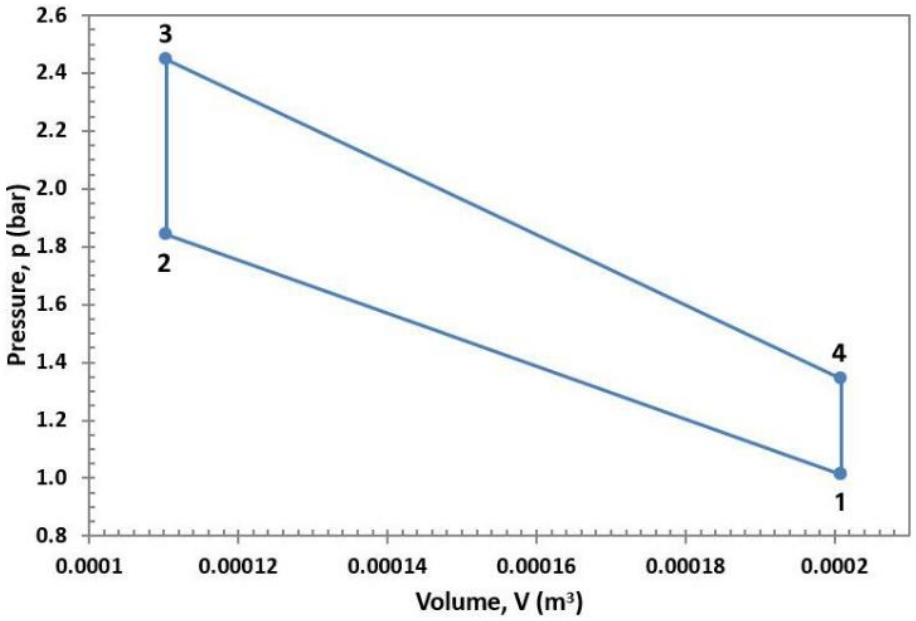

Figure 8: Ideal Stirling cycle p-V diagram

The relationship between pressure and volume in Figure 8 obtained after the pressure at each state is calculated using equations (9), (11), (15), and (16), and a relationship is made with V_{max} and V_{min}. Figure 8 is generated after conducting thermodynamic analysis in each process using equations (9), (11), and (15), then making a relationship with the maximum and minimum total volume that has been previously calculated. The initial pressure (p_1) is

the atmospheric pressure because there is no additional pressure outside the system. The pressure at point 2 (p_2) is obtained under isothermal conditions (process 1-2) of 1.843 bar. The pressure at point 3, which is the maximum pressure (p_3) generated by the Stirling engine during the testing process, is 2.446 bar. The pressure at point 4 (p_4) is 1.345 bar.

4.0 CONCLUSION

In this study, a prototype of the second-generation gamma Stirling engine was developed and tested. After analyzing the thermodynamic ideal cycle approach, the performance of the second Stirling engine is better than the previous generation. The thermal efficiency, engine rotational speed, ideal power, and Stirling engine pressure are all significantly reliant on the temperature differential between the hot and cold sides (ΔT) after testing and studying the 2nd generation Stirling engine. The three performance parameters have a higher value when ΔT is higher.

ACKNOWLEDGMENT

The authors would like to thank the Directorate General of Higher Education for financial support for the BPPDN scholarship that has been provided, the National Research and Innovation Agency for research assistance, and Mr Riclon H Sidabutar and the entire Stirling Engine Research Team in 2019 at the Medan Institute of Technology. The authors also thank the ICE-SEAM 2021 committee for accepting and providing the opportunity to present our work.

REFERENCES

[1] BPPT. (2018). Indonesia Energy Outlook 2018 (Yudiartono, Anindhita, A. Sugiyono, L. M. A.Wahid, & Adiarso (eds.)). Agency for the Assessment and Application of Technology. Available: https//www.bppt.go.id

[2] S. Aqilah, O. My, N. Saifuddin. "Non-Catalytic Microwave Assisted Transesterification of Palm Oil with Dimethyl Carbonate," *Journal of Mechanical Engineering and Technology*, vol. 12(1), 2020.

[3] B. Heidary, S. R Hassan-beygi, B. Ghobadian. "Investigating A Power Tiller Vibration Transmissibility Using Diesel-Biodiesel Fuel Blends on Stationary Conditions," *Journal of Mechanical Engineering and Technology*, vol. 5(1), pp. 19–31, 2013.

[4] Zainuddin, J. Nurdin, E. Is. "The Heat Exchanger Performance of Shell and Multi Tube Helical Coil as a Heater through the Utilization of a Diesel Machine's Exhaust Gas," *Aceh International Journal of Science and Technology*, vol. 5(1), pp. 21–29, 2016.

[5] Zainuddin, Eswanto, Jufrizal, Mulyadi, Barita, & A. Nasution."The effect of heat, air mass flow rate and temperature on paddy drying time using rotary type dryer," IOP Conference Series: Materials Science and Engineering, vol. 420(1), 2018.

[6] ACEEE. Emerging Technologies & Practices: Residential Micro-Cogeneration Using Stirling Engines, 2004.

[7] J. Harrison, E. On. Stirling engine systems for small and micro combined heat and power (CHP) applications. In Small and Micro Combined Heat and Power (CHP) Systems: Advanced Design, Performance, Materials and Applications ,pp. 179–205, Woodhead Publishing Limited, 2011.

[8] Jufrizal, F. H Napitupulu, Ilmi, H. Ambarita. "Manufacturing and testing prototype of a gamma type Stirling engine for micro-CHP application," IOP Conference Series:Materials Science and Engineering, vol. 725(1),pp. 1–9, 2020.

[9] T. Kaarsberg, A. Deppe, S. Kumar, A. Rosenfeld, J. Romm, L. Gielen. "Combined Heat and Power for Saving Energy and Carbon in Residential Buildings," *Building Industry Trends*, vol. 10, pp. 149–159, 2000.

[10] N. G Kirillov. "Power units based on Stirling engines: New technologies based on alternative fuels" *Russian Engineering Research*, vol. 28(2), pp. 104–110, 2008.

[11] D. Scarpete, K. Uzuneanu, N. Badea. "Stirling engine in residential systems based on renewable energy," 4th WSEAS International Conference on Energy Planning, Energy Saving,Environmental Education, EPESE'10, 4th WSEAS International Conference on Renewable Energy Sources, RES '10, January 2015,pp. 124–129.

[12] United Technologies Research Center. Micro-CHP Systems for Residential Applications, Issue June, 2006.

[13] P.K Aagade, A.P Rastogi, R.K Choudhary."Review : "Design and Development of Gamma Type Stirling Engine for Waste Heat Recovery," *International Journal of Science Technology & Engineering*, vol. 2(2),pp. 94–99, 2015.

[14] I. Arashnia, G. Najafi, B. Ghobadian, T. Yusaf, R. Mamat, M. Kettner. "Development of Micro-scale Biomass-fuelled CHP System Using Stirling Engine," *Energy Procedia*, vol. 75, pp. 1108–1113, 2015.

[15] C. Bachelier. *Stirling engines A technology overview*. In Royal Institute of Technology Stockholm, Sweden (Issue July), 2009.

[16] E. Cardozo, C. Erlich, A. Malmquist, L. Alejo. "Integration of a wood pellet burner and a Stirling engine to produce residential heat and power," *Applied Thermal Engineering*, vol 73(1), pp. 671–680, 2014.

[17] C. Çinar, H. Karabulut. "Manufacturing and testing of a gamma type Stirling engine," *Renewable Energy*, vol. 30(1),pp. 57–66, 2005.

[18] Damirchi, Hojjat, G. Najafi, S. Alizadehnia, B. Ghobadian, B., T. Yusaf, R. Mamat. "Design, Fabrication and Evaluation of Gamma-Type Stirling Engine to Produce Electricity from Biomass for the Micro-CHP System," *Energy Procedia*, vol. 75, pp. 137–143, 2015.

[19] Damirchi, Hojjatollah, G. Najafi, S. Alizadehnia, R. Mamat, C.S Nor Azwadi, W.H Azmi, M. M Noor. "Micro Combined Heat and Power to provide heat and electricalpower using biomass and Gamma-type Stirling engine," *Applied Thermal Engineering*, vol. 103, pp. 1460–1469, 2016.

[20] T. Finkelstein, A. J Organ, Air Engines. ASME Press, 2001.

[21] I. Kolin, S. Koscak-kolin, M. Golub. "Geothermal Electricity Production by Means of the Low Temperature Difference Stirling Engine," Proceedings World Geothermal Congress 2000, pp. 3199–3203, 2000.

[22] B. Kongtragool, S. Wongwises. "Performance of low-temperature differential Stirling engines," *Renewable Energy*, vol. 32, pp. 547–566, 2007.

[23] K. Kraitong, K. Mahkamov. "Optimization of Low Temperature Difference Solar Stirling Engines using Genetic Algorithm," Proceedings of the World Renewable Energy Congress–Sweden,pp. 3945–3952, 2011.

[24] A. Wagner. Calculations and experiments on y-type Stirling engines (Issue March). University of Wales, Cardiff, 2008.

[25] K. Wang, S.R Sanders, S. Dubey, F. Hoong, F. Duan, "Stirling cycle engines for recovering low and moderate temperature heat : A review," *Renewable and Sustainable Energy Reviews*, vol. 62, pp. 89–108, 2016.

[26] R. Gheith, F. Aloui, S. Ben Nasrallah. "Determination of adequate regenerator for a Gamma-type Stirling engine," *Applied Energy*, vol. 139, pp. 272–280, 2015.

[27] D. G Thombare, S.K Verma. "Technological development in the Stirling cycle engines," *Renewable and Sustainable Energy Reviews*, vol. 12(1), pp. 1–38, 2008.

[28] M.H Ahmadi, M.A Ahmadi, F. Pourfayaz. "Thermal models for analysis of performance of Stirling engine: A review," Renewable and Sustainable Energy Reviews, 68 (July2015), pp. 168–184, 2017.

[29] L. Grosu, C. Dobre, S. Petrescu."Study of a Stirling engine used for domestic micro-cogeneration," Thermodynamic analysis and experiment, *International Journal of Energy Research*, vol. 39, pp. 1280–1294, 2015.

[30] N. Martaj, L. Grosu , P. Rochelle, P. Rochelle. "Exergetical analysis and design optimization of the Stirling engine," *International Journal of Exergy*, vol. 3(1), pp. 45–67, 2006.

[31] S.M.H Wan Dawi, M.M Othman, I. Musirin, A.A.M Kamaruzaman, A.M Arriffin, N.A Salim. "Gamma Stirling engine for a small design of renewable resource model," *Indonesian Journal of Electrical Engineering and Computer Science*, vol. 8(2), pp. 350–359,2017.

[32] Y.A Çengel & M.A Boles. Thermodynamics: An Engineering Approach (4 th ed). University of Nevada, 2004.

[33] H. Ambarita, E.Y Setyawan, S. Ginting, & W. Naibaho. "Performance of a small compression ignition engine fuelled by liquified petroleum gas," IOP Conference Series: Materials Science and Engineering, vol. 237(1), pp. 1–8, 2017.